

## Midinfrared intersubband absorption on AlGaN/GaN-based high-electron-mobility transistors

Daniel Hofstetter,<sup>a)</sup> Laurent Diehl, and Jérôme Faist

*University of Neuchâtel, Institute of Physics, 1 Rue A.-L. Breguet, Neuchâtel, CH 2000, Switzerland*

William J. Schaff, Jeff Hwang, and Lester F. Eastman

*Cornell University, 415 Phillips Hall, Ithaca, New York 14853*

Christoph Zellweger

*Department of Physics, IMO, EPFL, Ecublens, Lausanne, CH-1015, Switzerland*

Intersubband absorption measurements on two nominally undoped AlGaN/GaN-based high-electron-mobility transistors with different Al compositions in the barrier layer are presented. The first transistor with a barrier consisting of  $\text{Al}_{0.6}\text{Ga}_{0.4}\text{N}$  showed an absorption peak at 247 meV ( $1973\text{ cm}^{-1}$ ) with a full width at half maximum (FWHM) of 126 meV, while the second device utilizing an  $\text{Al}_{0.8}\text{Ga}_{0.2}\text{N}$  barrier had its peak at 306 meV ( $2447\text{ cm}^{-1}$ ) with a FWHM of 86 meV. Self-consistently computed potentials and intersubband transition energies showed good agreement with the experimental findings, and therefore confirmed previously published values for the internal piezoelectric field in such structures.

During the last couple of years, the III nitrides have attracted a lot of attention as material for short wavelength diode lasers and also for high power electronic devices.<sup>1,2</sup> More recently, experiments dealing with optical intersubband transitions have been carried out and led to first promising results. Intersubband transitions on visible light emitting diodes have been reported<sup>3</sup> and Gmachl *et al.* measured optical intersubband absorption on specifically designed material at 1.7 and 1.55  $\mu\text{m}$ .<sup>4,5</sup> Optical intersubband absorption at a wavelength of 4  $\mu\text{m}$  has also been observed on AlGaN/GaN superlattices by Iizuka *et al.*<sup>6</sup> The reason why the nitrides are an interesting material for light emitters based on intersubband transitions is their high conduction band discontinuity.<sup>7,8</sup> The latter could eventually lead to light emission in the commercially interesting wavelength range around 1.55  $\mu\text{m}$ . One of the key features is the large lattice mismatch between GaN and its related compounds InGaN and AlGaN. More particularly, if AlGaN is grown on a thick GaN layer, then the lattice mismatch between GaN and AlGaN results in a tensile strained AlGaN layer. Since III nitrides grown on sapphire have a hexagonal crystal structure, the centers of gravity for the positive and negative charges within the crystal separate as soon as pressure is applied onto the lattice.<sup>9</sup> On an atomic scale, electrical dipoles are formed; and these add up to a large piezoelectric field at the heterointerface.<sup>10,11</sup> This feature of the AlGaN/GaN material system is advantageously used for the fabrication of high-electron-mobility transistor (HEMT) structures: the piezoelectric field induces a two dimensional electron gas (2DEG) at the AlGaN/GaN interface. This 2DEG can be depleted or enhanced using a Schottky gate contact; the 2DEG acts then as barrier layer of a field effect transistor.<sup>12</sup> With the triangular well formed at the AlGaN/GaN interface being relatively

deep, intersubband transitions at midinfrared wavelengths can be observed. Thanks to the piezoelectric field and the single heterointerface forming together the triangular well, one could hope to observe narrower spectral linewidths than when using rectangular wells with two barrier layers and thus two interfaces. In this letter, we will therefore present transmission measurements of such intersubband transitions for two different HEMT structures. Similar experiments have been performed on Si inversion layers,<sup>13,14</sup> and on modulation doped GaAs/AlGaAs structures.<sup>15</sup> By performing self-consistent calculations of the potential and the electron distribution at the interface, we will furthermore gain information about the size of the internal piezoelectric field.

Fabrication of these samples relied on molecular beam epitaxy on a C-face sapphire substrate. Growth started with 200 Å of pure AlN, and continued with a 1.2- $\mu\text{m}$ -thick nominally undoped GaN buffer layer, on top of which an undoped 150-Å-thick  $\text{Al}_x\text{Ga}_{(1-x)}\text{N}$  barrier layer was grown. The top layer, finally, was an undoped GaN contact layer with a thickness of 20 Å. Two different samples were investigated; sample GS1274 had an Al mole fraction of  $x=0.6$ , while the second sample, GS1282, had an Al content of  $x=0.8$ . Capacitance-voltage (C-V) measurements revealed that the thickness of the two uppermost layers, which corresponds to the position of the 2DEG, was 170 and 150 Å for the 60% and the 80% AlGaN samples, respectively. After growth of these structures, we cleaved rectangular pieces with a size of about  $4 \times 10\text{ mm}^2$ . The back and the two long sides were polished to optical mirror quality. The inset of Fig. 1 (bottom) shows a schematic side view of the resulting multipass waveguide. Its parallelogram-shaped cross section enables efficient in- and outcoupling of the light. A Ti/Pd/Au-based (1/40/500 nm) Schottky contact for the gate and Ti/Al-based (40/400 nm) ohmic contacts for source/drain were then deposited by lift-off on the top surface. Since the

<sup>a)</sup>Electronic mail: daniel.hofstetter@unine.ch

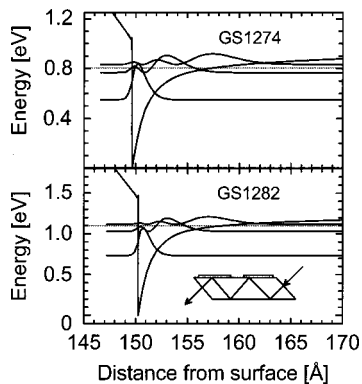


FIG. 1. Self-consistent calculation of the triangular potential well for the sample with 60% Al in the barrier (top), and with 80% Al in the barrier (bottom). The inset of the bottom figure shows a cross section through the multi pass waveguide. The dashed lines are the Fermi levels of the two devices.

structure was not used as a transistor, source and drain contacts were short circuited. The ohmic contact was annealed for 30 s under a  $N_2$  ambient and at  $700^\circ\text{C}$ . The total size of the gate contact was  $0.8 \times 3 \text{ mm}^2$  with the length corresponding to the width of the polished bar.

Figure 1 shows, for both samples, the self-consistently calculated potentials with the three lowest bound states in the triangular well. Transition energies of  $E_{21} = 222 \text{ meV}$  ( $1776 \text{ cm}^{-1}$ ),  $E_{31} = 288 \text{ meV}$  ( $2304 \text{ cm}^{-1}$ ) for GS1274, and of  $E_{21} = 297 \text{ meV}$  ( $2376 \text{ cm}^{-1}$ ),  $E_{31} = 383 \text{ meV}$  ( $3064 \text{ cm}^{-1}$ ) for GS1282 are predicted. Although the Schottky contacts for the two samples were of slightly different composition (GS1274 without Ti, GS1282 with Ti layer), we assumed for the two cases an equivalently calculated barrier height of  $1 \text{ eV} + 1.9 \text{ eV} \times p$  (with  $p$  being the Al mole fraction).

For the transmission experiment, a Fourier-transform infrared spectrometer was used (Nicolet 800). Since we did not see a difference between cryogenic temperatures and 300 K, all measurements were done at 300 K. The light of the internal infrared light source (glow bar) was sent across the multipass waveguide using a beam condenser ( $f/1.00$ ) and detected by the internal liquid nitrogen-cooled HgCdTe detector of the spectrometer. In agreement with the formula  $\Delta T/T = (T(V_{GS1}) - T(V_{GS2}))/T(V_{GS1})$ , where  $T(V_{GSi})$  is the transmission at the respective gate-source voltage  $V_{GSi}$ , a differential transmission signal was obtained by applying alternatively two different gate-source voltages.<sup>16</sup> In order to obtain a better signal-to-noise ratio, detection was performed in lock-in technique at a frequency of 15 kHz and a duty cycle of 50%. For the determination of the absolute magnitude of the differential transmission, we also measured some reference spectra on each sample using constant voltages. When applying a positive gate-source voltage on sample GS1274, we could go up to +2 V without seeing any noticeable leakage current; GS1282, on the other hand, showed up to 5 mA leakage current when applying a gate-source voltage of +2.5 V. A possible reason for the leakage of the 80% AlGaIn sample is that its barrier layer thickness is very close to the critical thickness; resulting in cracks. Since the area of our devices is relatively large, leakage paths due to these cracks are rather likely.

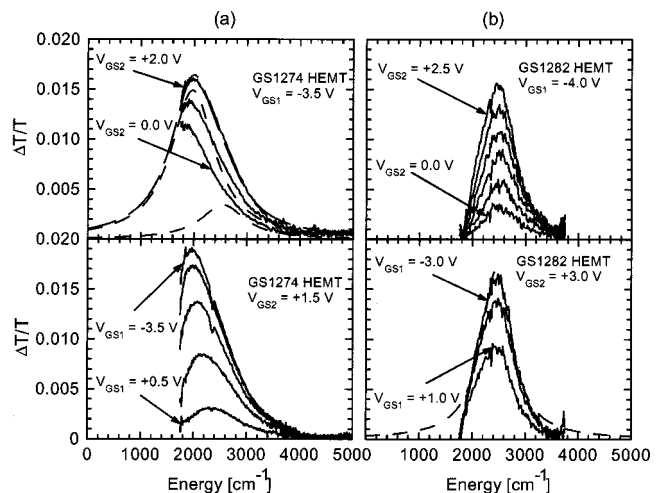


FIG. 2. (a) Differential transmission spectra of the  $\text{Al}_{0.6}\text{Ga}_{0.4}\text{N}/\text{GaN}$ -based HEMT sample GS1274 at 300 K. The three curves in the top figure were measured with a fixed  $V_{GS1} = -3.5 \text{ V}$ , along with three different values of  $V_{GS2}$  (0.0, +1.0, and +2.0 V). The fit in the top figure shows the two Lorentzians (short dashes) forming together the fit for the curve at  $V_{GS1} = -3.5 \text{ V}/V_{GS2} = +2.0 \text{ V}$  (long dashes). For the five curves in the bottom figure, we set five different values of  $V_{GS1}$  (-3.5, -2.5, -1.5, -0.5 and +0.5 V) and applied a voltage  $V_{GS2} = +1.5 \text{ V}$ . (b) Differential transmission spectra of an  $\text{Al}_{0.8}\text{Ga}_{0.2}\text{N}/\text{GaN}$ -based HEMT structure at 300 K. The six curves in the top figure were measured with a  $V_{GS1} = -4.0 \text{ V}$ , while utilizing six different values of  $V_{GS2}$  (0.0, +0.5, +1.0, +1.5, +2.0, and +2.5 V). For the three curves in the bottom figure, three different values for  $V_{GS1}$  (-3.0, 0.0, and +1.0 V) and a constant voltage  $V_{GS2} = +3.0 \text{ V}$  were applied. The fit (dashed line) in the bottom figure is performed on the  $V_{GS1} = -3.0 \text{ V}/V_{GS2} = 3.0 \text{ V}$  curve and consists of a single Lorentzian peak.

In the upper half of Fig. 2(a), we present a series of transmission spectra for the sample with 60% Al content (GS1274). The three curves were measured with a constant  $V_{GS1} = -3.5 \text{ V}$  while using three different  $V_{GS2}$ .  $V_{GS1}$  was set as the voltage at which the signal started to saturate. Since sapphire absorbs heavily for energies below  $1670 \text{ cm}^{-1}$ , this part of the spectra could not be observed. For an increasingly positive  $V_{GS2}$ , we saw a small shift of the peak from  $1775 \text{ cm}^{-1}$  at 0.0 V up to  $1975 \text{ cm}^{-1}$  at +2.0 V. This shift is, at least qualitatively, consistent with the expected behavior of the triangular well under application of an external voltage: a positive voltage makes the well deeper, which will shift the peak towards higher energy. A computation of the transition energies for GS1274 at different gate-source voltages,  $V_{GS}$ , showed a nearly linear dependence following roughly the relation  $\Delta E_{21}(V_{GS}) = 235 \text{ meV} + 14.5 \text{ meV/V} \times V_{GS}$ . We see experimental wavelength shifts which are slightly smaller than the ones predicted by the above formula (linear term  $12.5 \text{ meV/V}$  instead of  $14.5 \text{ meV/V}$ ).

For the five spectra at the bottom of Fig. 2(a), we used five different values of  $V_{GS1}$ , while setting  $V_{GS2} = +1.5 \text{ V}$ . Therefore, we measured the differential transmission of a less and less depleted well, which manifests itself in a wavelength shift towards higher energies, up to  $2300 \text{ cm}^{-1}$ . As mentioned earlier, the differential signal started to saturate when applying a gate-source voltage  $V_{GS1} < -3.5 \text{ V}$ . When comparing the sheet carrier density (from the  $C-V$  measurement) as a function of voltage with the integrated area of the curves at the bottom Fig. 2(a), we found good agreement.

Furthermore, the observed carrier density saturation at  $-4.0$  V is a good indication for an almost complete depletion of the well at  $V_{GS} = -3.5$  V. The high energy shoulder of the peaks in Fig. 2(a) is not inconsistent with the assumption of having transitions from two different excited states to the ground state. We therefore performed a fit on the uppermost curve of Fig. 2(a) (top) using two Lorentzian peaks. The computed oscillator strength ratio of the involved transitions ( $f_{31}/f_{21}=0.23$ ) determined the respective height of the Lorentzians. The common width of the two peaks as well as their position and size were used as the four fit parameters. This procedure yielded the dashed line of Fig. 2(a) (top). Also shown are the two single Lorentzians (short dashes) which contribute to the total signal. Transition energies of  $E_{21}=247$  meV ( $1973$   $\text{cm}^{-1}$ ) and  $E_{31}=318$  meV ( $2547$   $\text{cm}^{-1}$ ) are obtained. The peak width [full width at half maximum (FWHM)] is  $\Delta E_{21}=\Delta E_{31}=126$  meV ( $1004$   $\text{cm}^{-1}$ ). Most likely, a small error in the Al composition was at the cause of the  $+10\%$  difference between theoretical and experimental transition energies. For both measurement series presented in Fig. 2(a), the signals were purely TM polarized. This was partly due to the intersubband nature of the electronic transition involved; but resulted also from the close proximity of the 2DEG to the metal layers on the surface, which dictates the electric field component in the growth direction be maximal at the wafer surface.

Looking at the top of Fig. 2(b), we see the analogous measurement to the one presented in Fig. 2(a) (top), but this time with sample GS1282. As expected, the peak is now at a higher energy, namely at  $306$  meV; corresponding to  $2447$   $\text{cm}^{-1}$ . Its FWHM is smaller than the one of GS1274, namely only about  $86$  meV ( $685$   $\text{cm}^{-1}$ ). Both width and transition energy are comparable (but not smaller) to the best ones reported in Ref. 4 on an AlGaIn/GaN based super lattice. The series consisting of six curves was measured at a constant  $V_{GS1} = -4.0$  V, and six different  $V_{GS2}$  values. The wavelength shift which was quite pronounced in Fig. 2(a) was completely absent this time. If we look finally at the lower half of Fig. 2(b), where three different  $V_{GS1}$  values, along with a constant value of  $V_{GS2} = +3.0$  V was used, then we observe again no significant wavelength change. For the strongest absorption signal in Fig. 2(b) (bottom), we performed a similar fit as with GS1274. Although the computed ratio of the dipole matrix elements was comparable to the first HEMT, we found this time no evidence for a second Lorentzian peak.

An analysis of the results obtained with the two samples reveals that the positions of the principal absorption peaks agreed quite well with the self-consistent computation. The errors in transition energy of  $+10\%$  for GS1274 and  $+3\%$  for GS1282 can be explained by a slightly too high Al content of the AlGaIn barrier layers. Since these layers are only  $150$  Å thick, their Al composition is rather difficult to measure by x-ray diffraction. For sample GS1274, we even have evidence of seeing a transition from the second excited state to the ground level; and its tuning behavior agrees reasonably well with the computation. Why did we not observe the latter two effects on GS1282 which, from a linewidth point of view, looked even better than GS1274? In our structures,

the triangular well has a “thickness” comparable to one atomic repeat distance ( $5$  Å). Thus, the main assumption of the envelope function approximation (EFA), namely that the wave function varies slowly with respect to the periodic lattice potential, is not fulfilled. Since the terms “triangular well” or “square well” become almost meaningless if the well thickness approaches one monolayer, it is no surprise that the Stark tuning was not consistently observed. Although the transition energies were correctly predicted, the EFA might have reached its limits for this application.

Of course, it cannot be ruled out that some interfacial roughness or cracking has nevertheless affected the optical properties of GS1282. After all, the Hall effect measurement of this sample showed a considerably smaller sheet carrier density than expected (only  $2.48 \times 10^{13}$   $\text{cm}^{-2}$  instead of  $3.9 \times 10^{13}$   $\text{cm}^{-2}$ ). In contrast to this, GS1274 revealed a measured sheet carrier density of  $n_s = 2.01 \times 10^{13}$   $\text{cm}^{-2}$  which corresponded to the calculated one of  $2.6 \times 10^{13}$   $\text{cm}^{-2}$ . By taking into account the total area of the GS1274 absorption peak ( $3.44 \times 10^{-3}$  eV), the dipole matrix element of the involved transition ( $6.1$  Å), and the different geometric parameters ( $N_{\text{wells}}=1$ ,  $N_{\text{passes}}=6$ ) of the polished bar, we could once more determine the value of  $n_s$ . This yielded a value of  $2.04 \times 10^{13}$   $\text{cm}^{-2}$ ; in excellent agreement with the Hall effect measurement. The dipole matrix element was computed using an effective mass of  $m^* = 0.262m_e$ .

In conclusion, we have presented differential transmission measurements on two different HEMT structures. An intersubband transition between the two lowest subbands of the triangular well was seen. We found good agreement between self-consistently computed and experimentally determined transition energies, thus confirming previously published values of the internal piezofield.

The authors acknowledge help from Xavier Niquille and Sébastien Dubail at the University of Neuchâtel. This work was supported by the NICOP and MURI programs, both of the Office of Naval Research.

- <sup>1</sup>S. Nakamura, M. Senoh, S. Nagahama, N. Iwasa, T. Yamada, T. Matsushita, H. Kiyoku, Y. Sugimoto, T. Kozaki, H. Umemoto, M. Sano, and K. Chocho, *Appl. Phys. Lett.* **73**, 832 (1998).
- <sup>2</sup>Y.-F. Wu, B. P. Keller, S. Keller, D. Kopolnek, P. Kozodoy, S. P. Denbaars, and U. K. Mishra, *Appl. Phys. Lett.* **69**, 1438 (1996).
- <sup>3</sup>D. Hofstetter, J. Faist, and D. P. Bour, *Appl. Phys. Lett.* **76**, 1495 (2000).
- <sup>4</sup>C. Gmachl, H. M. Ng, and A. Y. Cho, *Appl. Phys. Lett.* **77**, 334 (2000).
- <sup>5</sup>C. Gmachl, H. M. Ng, S.-N. G. Chu, and A. Y. Cho, *Appl. Phys. Lett.* **77**, 3722 (2000).
- <sup>6</sup>N. Iizuka, K. Kaneko, N. Suzuki, T. Asano, S. Noda, and O. Wada, *Appl. Phys. Lett.* **77**, 648 (2000).
- <sup>7</sup>J. Faist, F. Capasso, C. Sirtori, D. L. Sivco, J. N. Baillargeon, A. L. Hutchinson, and A. Y. Cho, *Appl. Phys. Lett.* **68**, 3680 (1996).
- <sup>8</sup>C. Sirtori, P. Kruck, S. Barbieri, P. Collot, J. Nagle, M. Beck, J. Faist, and U. Oesterle, *Appl. Phys. Lett.* **73**, 3486 (1998).
- <sup>9</sup>R. C. Powell, N.-E. Lee, Y.-W. Kim, and J. E. Greene, *J. Appl. Phys.* **73**, 189 (1993).
- <sup>10</sup>S.-H. Park and S.-L. Chuang, *Appl. Phys. Lett.* **72**, 3103 (1998).
- <sup>11</sup>H. S. Kim, J. Y. Lin, H. X. Jiang, W. W. Chow, A. Botchkarev, and H. Morkoç, *Appl. Phys. Lett.* **73**, 3426 (1998).
- <sup>12</sup>R. M. Chu, Y. G. Zhou, Y. D. Zhang, P. Han, B. Shen, and S. L. Gu, *Appl. Phys. Lett.* **79**, 2270 (2001).
- <sup>13</sup>T. Ando, A. B. Fowler, and F. Stern, *Rev. Mod. Phys.* **54**, 437 (1982).
- <sup>14</sup>D. Heitmann and U. Mackens, *Phys. Rev. B* **33**, 8269 (1986).
- <sup>15</sup>E. Batke, G. Weimann, and W. Schlapp, *Phys. Rev. B* **39**, 11171 (1989).
- <sup>16</sup>J. Faist, F. Capasso, C. Sirtori, D. L. Sivco, A. L. Hutchinson, S. N. G. Chu, and A. Y. Cho, *Appl. Phys. Lett.* **65**, 94 (1994).